Biosensors and Bioelectronics 287 (2025) 117651

Contents lists available at ScienceDirect

Biosensors and Bioelectronics

journal homepage: www.elsevier.com/locate/bios

A CRISPR/Cas12a-powered liquid crystal aptasensor for point-of-care detection of prostate-specific antigen for early-stage cancer diagnosis

Zahra Khoshbin [a,b,c], Elham Sameiyan [a,b], Fatemeh Alizadeh [d,e], Mohammad Ramezani [c], Mona Alibolandi [c], Khalil Abnous [c,d,*], Seyed Mohammad Taghdisi [a,b,**]

[a] Targeted Drug Delivery Research Center, Pharmaceutical Technology Institute, Mashhad University of Medical Sciences, Mashhad, Iran
[b] Department of Pharmaceutical Biotechnology, School of Pharmacy, Mashhad University of Medical Sciences, Mashhad, Iran
[c] Pharmaceutical Research Center, Pharmaceutical Technology Institute, Mashhad University of Medical Sciences, Mashhad, Iran
[d] Department of Medicinal Chemistry, School of Pharmacy, Mashhad University of Medical Sciences, Mashhad, Iran
[e] Surgical Oncology Research Center, Mashhad University of Medical Sciences, Mashhad, Iran

ARTICLE INFO

Keywords:
Aptamer
Biosensor
Palindromic repeats
Cas12a protein
Prostate cancer
Liquid crystal
Portable

ABSTRACT

Herein, an ultrasensitive aptasensor was developed for monitoring prostate-specific antigen (PSA) levels for the first time by incorporating the catalytic activity of CRISPR/Cas12a assembly and directional orientation of liquid crystal (LC) molecules. In the absence of PSA, the specific aptamer was hybridized with crRNA segment of the CRISPR/Cas12a assembly, which activated it for cleaving the ssDNA strand on the sensing substrate. This resulted in a dark background of the sensing substrate. While the assembly was unable to cleave the ssDNA sequence in the presence of PSA, due to forming the PSA-aptamer hybrid and disabling the enzymatic assembly, visualizing the colorful polarized sensing substrate. By changing the polarized background of the LC aptasensor from murky to multicolored, PSA could be detected ranging from 1 ag mL^{-1}-1 pg mL^{-1} and 1 pg mL^{-1}-1 ng mL^{-1} with a detection limit of 0.28 ag mL^{-1}. With the potency to determine PSA in the spiked human serum samples with the recovery amounts of 97.87–99.57 %, the CRISPR/Cas12a-powered LC aptasensor is a reliable test kit for cancer screening. This was also confirmed by comparing the results obtained from the LC aptasensor with those of ELISA analysis for human serum samples of some patients. Being ultrasensitive, cost-effective, label-free, and user-friendly, the aptasensor can be an efficient future portable gadget for early-stage cancer monitoring.

1. Introduction

Early detection of cancer before metastasis to other organs is one of the most important objections in cancer diagnosis. Biomarkers can act as molecular signatures of a particular illness, detectable at various concentrations in urine, blood, saliva, and tissue. The recognition of biomarkers can be a reliable approach for detecting diseases at an early stage that are triggered by them. By utilizing such a forecast, it is possible to enhance the effectiveness of treatments (Edwards et al., 2005; Ludwig and Weinstein, 2005). Prostate cancer is reported as a prevalent malignancy among men, the sixth leading cause of cancer in middle-aged men from 45 to 60 years (Adamaki and Zoumpourlis, 2021; Sekhoacha et al., 2022). The efficacy of treatment for late-stage prostate cancer is reduced, leading to a higher likelihood of recurrence in patients diagnosed at an advanced stage (Etzioni et al., 2003; Nakhjavani et al., 2023). Prostate-specific antigen (PSA) is primarily produced by the prostate gland. It has been recognized as a key biomarker for prostate cancer and is closely linked to patient outcomes following treatment for the disease (Lilja et al., 2008; Madu and Lu, 2010; Taghdisi et al., 2020b).

Hence, developing analytical approaches capable of sensitive PSA detection is very essential. Many traditional methods have been reported for PSA determination, including radioimmunoassays (Graves et al., 1992), immunosensors (Li et al., 2011), enzyme-linked immunosorbent arrays (Xuan et al., 2016), and surface-enhanced Raman scattering-incorporated procedures (Cheng et al., 2017). These methods

* Corresponding author. Department of Medicinal Chemistry. Pharmaceutical Research Center, Pharmaceutical Technology Institute, Mashhad University of Medical Sciences, Mashhad, Iran.
** Corresponding author. Department of Pharmaceutical Biotechnology. Targeted Drug Delivery Research Center, Pharmaceutical Technology Institute, Mashhad University of Medical Sciences, Mashhad, Iran.
E-mail addresses: abnouskh@mums.ac.ir (K. Abnous), taghdisihm@mums.ac.ir (S.M. Taghdisi).

https://doi.org/10.1016/j.bios.2025.117651
Received 20 July 2024; Received in revised form 26 May 2025; Accepted 31 May 2025
Available online 2 June 2025
0956-5663/© 2025 Elsevier B.V. All rights are reserved, including those for text and data mining, AI training, and similar technologies.

frequently rely on immune responses involving antibodies, which face challenges associated with their stability, storage, and alteration. Besides, these methods are inconvenient, labor-intensive, complicated, high-cost, time-consuming and operator-dependent (Li et al., 2023; Srivastava et al., 2018; Wei et al., 2023).

As superior sensing approaches, aptamer-included biosensors (aptasensors) have received extensive attention because of the benefits of great sensitivity, inexpensiveness, repeatability, rapid response, reliability, ease of operation, and great stability (Dadmehr et al., 2023; Gorgani et al., 2023). As the unique biological recognition elements, aptamers are single strands of RNA or DNA oligonucleotides in-vitro selected through SELEX process. They are known as nucleic acid analogs of antibodies, but with various structures and properties (Fang and Tan, 2010; Mohammadi et al., 2024b). Compared to traditional antibodies, aptamers are inherently non-immunogenic molecules that are suitable for in-vivo studies. In addition, they are chemically and thermally very stable and highly active even after denaturation. Unlike antibodies, they can be customized with different functional groups, tag molecules, etc. (Chen et al., 2023; Lee et al., 2010; Nguyen and Gu, 2023) For the first time, Savory et al. (2010) used a genetic algorithm as an post-SELEX screening approach to introduce an aptamer strand with improved specificity toward PSA molecule. As a result of this in silico maturation approach, a DNA aptamer was achieved with the high binding ability to PSA, 48-times more than that of the parent strand, applied in the different studies (Sánchez-Salcedo et al., 2022). According to its high affinity and great specificity toward PSA, the developed aptamer has been extensively applied to progress sensitive sensing assays for detection of PSA (Benvidi et al., 2018; Li et al., 2019; Souada et al., 2015; Taghdisi et al., 2020a, 2022a).

Today, assays for biosensing without the need for labels have advanced considerably as a fascinating choice for detecting targets. Due to the laborious, time-consuming, complicated, costly, and denaturing nature of the labeling process for biomolecules, there has been significant focus on creating tag-free aptasensors to address these challenges (Forouzanfar et al., 2020; Jia et al., 2020; Mohammadi et al., 2024a; Song et al., 2022). The labeling process requires complex chemical synthesis and purification procedures for attaching tag molecules to aptamer strands. This process also adversely affects the aptamer affinity toward its target molecule. Furthermore, attaching signal reporter molecules covalently to guanine-rich aptamers disrupts the output signal by utilizing the quenching ability of the guanine base through photoinduced electron transfer from the labeled molecule to it (Charbgoo et al., 2016; Cui et al., 2016; Ma et al., 2021). In recent decades, liquid crystal (LC)-merged aptasensors have been of great interest as novel candidates for label-free optical biosensors due to facile operation, cost-effectiveness, rapid determination function, broad response range, and so on (Khoshbin et al., 2022a; Kim et al., 2019).

LCs are soft matters with unique properties of long-range order in orientation and fluidity. They also possess extremely low anchoring energy, rendering them highly responsive to external stimuli (Hussain et al., 2016). Based on the reorientation of LC molecules, these responsive materials are able to convert and amplify the interaction of target and aptamer into an optical signal visible through polarized light microscopy. As extraordinary sensing tools, LC aptasensors allow events occurring at the nanoscale to be simply detected even with the naked eye; and they are user-friendly devices, preventing expensive, operator-dependent, and complex laboratory equipment (Wang et al., 2017; Zhang et al., 2018). Furthermore, these innovative aptasensing tools can be coupled with smartphones to achieve promising lab-on-chip gadgets for on-site and real-time applications in people's daily life and the industrial world (Nandi and Pal, 2018).

Clustered regularly interspaced short palindromic repeats (CRISPR)-guided proteins (Cas), together abbreviated as CRISPR/Cas systems, represent a groundbreaking technology in the realms of biosensing assays, adaptive transcriptional regulation, and programmable genome editing (Cong et al., 2013; Cong and Zhang, 2015). These platforms have garnered attention in recent times because of their characteristics, such as customizable structure, simple customization, easy use, excellent compatibility with living organisms, straightforwardness, and collateral cleavage activity (Abnous et al., 2021a; Kadam et al., 2023; Khoshbin et al., 2022b). Among CRISPR/Cas assemblies, Cas12a has proven to be a highly effective instrument for creating biosensors with enhanced sensitivity (Abnous et al., 2021b; Taghdisi et al., 2022b; Wu et al., 2023). CRISPR/Cas12a is equipped with both a RNA-guided DNase function for cutting target DNA (cis-cleavage) and a non-selective single-stranded DNase function (trans-cleavage) when target DNA is recognized by the associated crRNA in a controlled manner (Dehghani et al., 2018; Li et al., 2018). CRISPR/Cas12a assemblies are potent to be unified in various aptasensing arrays for detecting a wide range of targets, such as viruses, bacteria, cancer biomarkers, toxins, narcotics, food pollutants, metal ions, and so on (Hajikhani et al., 2023; Haowei et al., 2023; Zavvar et al., 2022). Hence, a combination of aptamer science, LC technology, and CRISPR/Cas technique can remarkably provide a new pathway toward real-time and on-site target recognition. For the first time, we introduced a CRISPR/Cas12a boosted LC aptasensor with a new design for ultrasensitive detection of PSA biomarker based on the change in the homeotropic alignment of LCs directly controlled by the immobilized ssDNA strands on the glass substrate after the catalytic function of CRISPR/Cas12a assembly. The novel LC aptasensing platform reinforced by CRISPR/Cas12a assembly could monitor PSA biomarker at the ag mL^{-1} levels. This allows the researcher in the clinic to eliminate the effects of interfering factors such as proteins and blood fats just by diluting the serum samples, which reduces the possible errors in detection process.

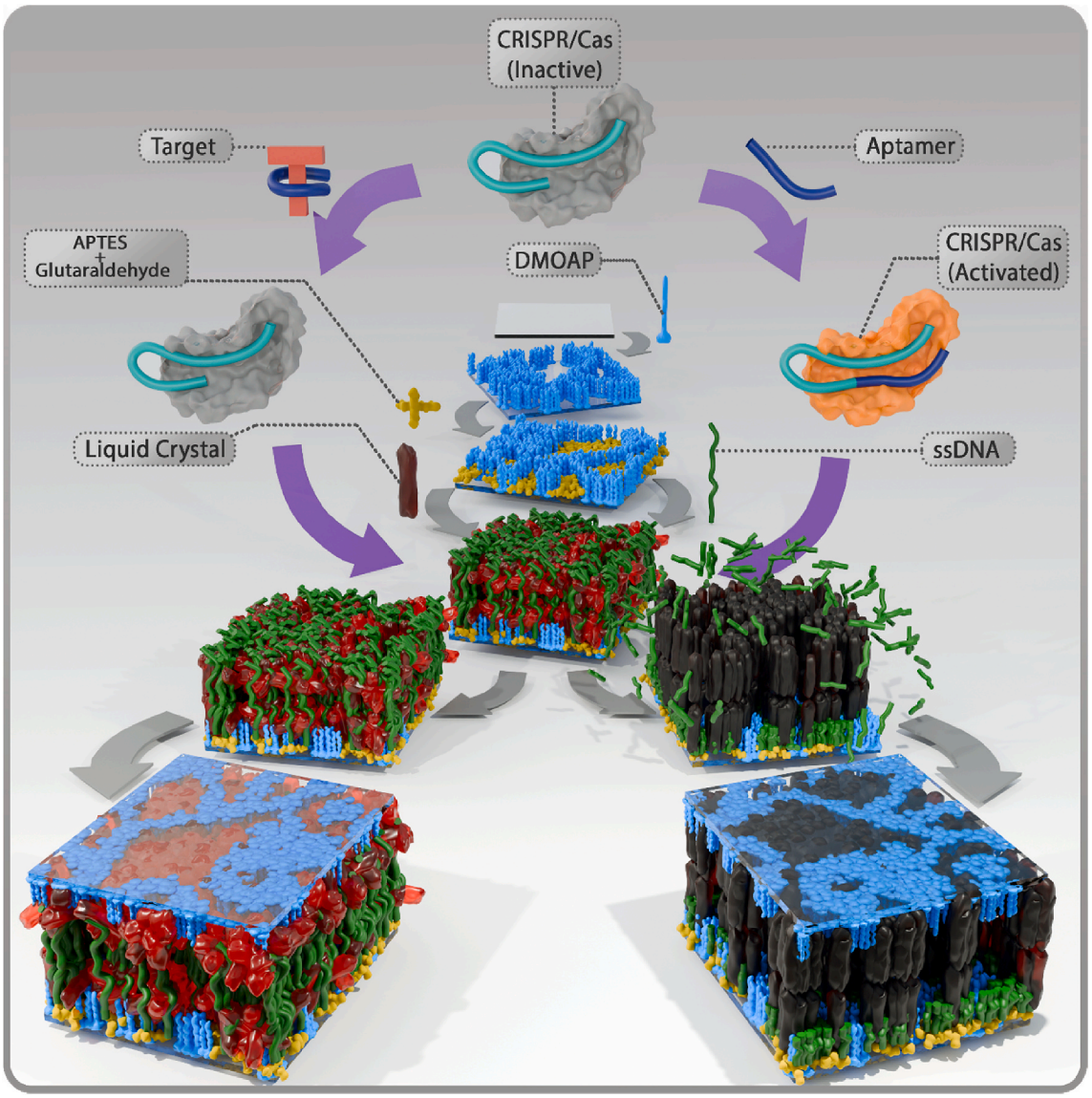
2. Experimental part

The details of the experimental tests are included in the 'Supporting Information' file.

3. Results and discussions

3.1. Detection mechanism

Scheme 1 clarifies the identifying principle of the CRISPR/Cas12a-powered LC aptasensor for PSA detection. Treating the glass substrate with Piranha solution inserted hydroxyl (-OH) groups on it for subsequent attachment of APTES molecules. The molecules were immobilized on the glass substrate by forming Si-O bridge on it. With leaving free amine (-NH_2) groups, APTES molecules could be an anchorage for GL linkers through trapping their aldehyde (-CHO) groups (Syga et al., 2018). Finally, the amine-modified ssDNA was attached onto the APTES-treated glass by interacting with free -CHO segment of GL linker (Wu et al., 2018). In the absence of PSA, the specific aptamer was hybridized with the crRNA strand and activated the Cas12a-crRNA system. It resulted in the trans-cleavage of the ssDNA on the sensing substrate, in addition to the cis-cleavage of the aptamer strand. With cleaving to short sequence with a length of about 5 base units (Khoshbin et al., 2023a), the remaining ssDNA on the detection surface, together with DMOAP as a control agent, caused the liquid crystals to align perpendicularly. As a result, a notably dark background was observed on the aptasensing substrate. By adding PSA, the aptamer was complexed with PSA, which prevented its hybridization with the crRNA strand. Consequently, the inactive Cas12a-crRNA system could not cleave the ssDNA sequence on the sensing platform. The intact ssDNA with a length higher than 24 base units disturbed the homeotropic direction of LCs to random (Verdian et al., 2023), which changed the polarized vision of the sensing platform from dark to chromatic.



Scheme 1. Schematic illustration of the LC aptasensor mediated by CRISPR/Cas12a assembly for ultrasensitive monitoring of PSA biomarker.

3.2. Optimization step

3.2.1. APTES and DMOAP amount

Since the amounts of DMOAP and APTES can affect the orientational direction of LCs, the glass substrate was modified with various amounts of the modifiers to determine the optimum value. Fig. S1 illustrates the polarized vision of the slides and their quantitative analysis. Based on Fig. S1, the completely murky background of the substrates was obtained by the APTES/DMOAP mixture with the volumetric ratio of 1:1 and less than that. A volumetric ratio of APTES/DMOAP more than 1:1 induced color background of the sensing substrates as a sign of perturbation in vertical order of LCs. Hence, the ratio of 1:1 was the optimum of the modifiers, resulting in the uniformly homeotropic alignment of LCs.

The DMOAP amount on the topcoat glass can also alter the arrangement of LCs (Khoshbin et al., 2022b). Fig. S2 shows the polarized view of glass substrates comprising the different amounts of DMOAP. As a result, a completely dark view of the substrate was attained by a DMOAP concentration of 0.35 % v/v, proving the perpendicular direction of LCs. Hence, it was the optimum for modifying the topcoat slide.

3.2.2. GL linker amount

Amount of GL molecule as bridge for fixing the aptamer on the glass platform can change the vertical direction of LCs (Verdian et al., 2022). Therefore, its optimum value was achieved by visualizing the platforms modified by the various amounts of GL, as depicted in Fig. S3. A dark view was obvious for the glass platform treated by GL with the concentration of 0.5 % v/v, which aligned all LCs homeotropically. Hence, it was specified as the optimum.

3.2.3. Concentration of ssDNA strand

To attain the highest efficiency of the designed aptasensor, it is requisite to have the maximum number of ssDNA strands on the sensing substrate for inducing the highest directional irregularity of LCs (Scheme 1). Hence, the concentration of ssDNA strand was optimized, as depicted in Fig. S4. It is evident that the intensity of the colored background on the substrate increased as the ssDNA concentration reached 200 nM, and remained stable when increased to 300 nM. This indicates that the most significant disruption in the vertical alignment of liquid crystals (LCs) occurred at an ssDNA concentration of 200 nM, which was deemed to be ideal.

3.2.4. Reaction buffer components and cleavage time for CRISPR/Cas12a assembly

The recent study proves that the components of the reaction buffer can affect the trans-cleavage catalytic efficiency of CRISPR-CA12a system (Deng et al., 2022). To have the highest cleavage potency of CRISPR/Cas12a assembly for ssDNA digestion, it is essential to apply the most efficient reaction buffer. Consequently, the optimal levels of DTT and PVA compounds were determined for the reaction buffer. At the same time, the ideal duration was identified to achieve the highest cleavage efficiency of CRISPR/Cas12a (referred to as cleavage time). For this aim, CRISPR/Cas12a assembly was prepared in a reaction buffer containing DTT (1 mM), NaCl (50 mM), $MgCl_2$ (15 mM), and Tris-HCl (10 mM, pH 7.5). After 20 min incubation time and centrifugation step, 10 μL of it was added to the aptamer solution (final concentration of 50 nM), injected onto the ssDNA-modified platform, and kept for 30 min. Visualizing the platform by a polarizing microscope highlighted that DTT with a concentration of 1 mM caused only 15 % darkness of the sensing platform (Fig. S5B). Moreover, extending the duration from 30 min to 2 h for cutting a greater quantity of ssDNA molecules did not impact the color intensity of the surface (Fig. S5C). The test was repeated for the system containing DTT (10 mM), NaCl (50 mM), $MgCl_2$ (15 mM), and Tris-HCl (10 mM, pH 7.5). The findings suggest that treating the platform with 10 mM of DTT and an incubation period of 30 min resulted in a 35 % increase in its darkness (Fig. S5D). The platform darkness remained unchanged with passing time from 30 min to 2 h, clarifying that increasing time had no effect on the cleavage potency of CRISPR/Cas12a assembly (Fig. S5E). In the following, a reaction buffer containing DTT (10 mM), PVA (1 % w/v), NaCl (50 mM), $MgCl_2$ (15 mM), and Tris-HCl (10 mM, pH 7.5) was applied for the test, which resulted in 75 % darkness of the sensing substrate (Fig. S5F). Extending the duration of the cleavage process from 30 min to 90 min resulted in the platform reaching 85 % darkness (Fig. S5G), with no further change observed thereafter (Fig. S5H). Through the utilization of DTT at a concentration of 20 mM in combination with 1 % w/v of PVA and a cleavage time of 30 min, a darkness level of 89 % was reached (see Fig. S5I). Extending the cleavage time to 45 min resulted in a consistently dark sensing platform, suitable for aligning all LCs vertically. Hence, a buffer reaction comprising DTT (20 mM), PVA (1 % w/v), NaCl (50 mM), $MgCl_2$ (15 mM), and Tris-HCl (10 mM, pH 7.5), and also, a cleavage time of 45 min was considered for the further tests.

3.2.5. Formation time of CRISPR/Cas12a assembly

In order to create the highest possible number of CRISPR/Cas12a assemblies, it is necessary to incubate the Cas12a protein with the crRNA sequence for an appropriate period of time. Hence, Cas12a (final concentration of 250 nM) and crRNA (final concentration of 500 nM) were mixed in the optimal reaction buffer, and incubated for different times (10, 20, and 30 min). After mixing with aptamer, injecting onto a ssDNA-modified platform, and allowing for a cleavage period of 45 min, the polarized perspective of the surface was captured, as shown in Fig. S6. The results prove that the most digestion of ssDNA strands was achieved for the formed CRISPR/Cas12a assembly during 20 min, inducing a completely dark platform. So, 20 min was chosen as the optimum time for the creation of the highest number of the assembly.

3.2.6. Cas12a and crRNA ratio

To have the highest trans-cleavage activity of CRISPR/Cas12a assembly, it is crucial to optimize the concentration ratio of Cas12a protein and crRNA strand. For this purpose, the different ratios of the components were applied to form CRISPR/Cas12a assembly; after mixing with the specific aptamer, the trans-cleavage potency was examined, as illustrated in Fig. S7. Based on Fig. S7, the murky platform was observed when the cleavage function was carried out by a CRISPR/Cas12a assembly with the Cas12a:crRNA concentration ratio of 1:2. As a result, the ratio of 1:2 was considered for forming the CRISPR/Cas12a assembly with the highest trans-cleavage enzymatic function.

3.2.7. Cas12a and crRNA concentration

One additional important factor was the adjustment of the levels of Cas12a protein and crRNA strand to maximize the catalytic efficiency of the CRISPR/Cas12a assembly. Hence, the different concentrations with the optimum Cas12a:crRNA concentration ratio were applied to form the assembly; and the results of trans-cleavage activity are given in Fig. S8. The results highlight that Cas12a with the concentration of 50 nM induced a completely dark substrate, and increasing the concentration beyond that point showing no impact on the darkness of the platform. This demonstrates that utilizing 50 nM of Cas12a protein and 100 nM of crRNA sequence was the optimal combination for constructing the assembly.

3.2.8. Aptamer concentration

The concentration of the aptamer can significantly impact the performance of the aptasensor. When the concentration exceeds the optimal level, the aptamer is left unbound in the solution. As a result, some of the catalytic function of the CRISPR/Cas12a system is utilized to cleave the unbound aptamers, leading to a decrease in its catalytic efficiency on the ssDNA strand, which is an unfavorable outcome. On the other hand, when the concentration of the aptamer falls below its ideal level, there are insufficient molecules available to bind with the crRNA strand and create the most effective CRISPR/Cas12a complex. As a result, a lower number of activated complexes leads to reduced trans-cleavage activity on the ssDNA sequence, which is an additional disadvantage. To optimize the aptamer concentration, CRISPR/Cas12a system was hybridized with the aptamer strand with the different concentrations, and applied for trans-cleavage activity. The results are given in Fig. S9, proving that the colored vision of the platform diminished by an increase in the aptamer concentration from 12.5 nM to 50 nM. A dark view of the sensing platform was obtained by applying 50 nM of the aptamer solution, confirming the complete cleavage of all ssDNA strands on the platform. Interestingly, an increase in the aptamer concentration more than 50 nM restored the color view of the substrate, proving a decrease in the catalytic function of CRISPR/Cas12a assembly by interference of the free aptamer strands. Therefore, 50 nM was the optimum aptamer concentration.

3.2.9. Target incubation time

In order for the aptasensor to function correctly, it is essential to allow sufficient time for PSA incubation to ensure optimal interaction between the aptamer and the target. If the incubation time of PSA is less than its optimal value, the maximum number of the aptamer-target complexes will not be formed. Consequently, the unbound aptamer strands will bind with the crRNA sequence, activating the CRISPR/Cas12a system. This activation causes the assembly cleaves ssDNA strands on the sensing substrate, resulting in an incorrect response of the aptasensor. Hence, different times were allocated for the incubation of PAS with the specific aptamer, and after adding to CRISPR/Cas12a assembly, the cleavage process was proceeded on the sensing substrate. The polarized vision of the substrate is indicated in Fig. S10, illustrating that the brightness of the material decreased over time up to 30 min, and then stabilized. This demonstrates that a 30-min incubation period is necessary for optimal capture of the aptamer strands through full interaction with all PSA molecules.

3.3. Detection of PSA molecules

The aptasensor's ability to detect PSA was assessed across different concentrations. The polarized illustration of the sensing platform after analyzing the PSA concentrations is shown in Fig. 1. The results clarify an increase in the color mode of the aptasensing platform by changing the PSA concentrations from 1 ag mL^{-1} to 1 ng mL^{-1}. Clearly, as the level of PSA increases, there is a corresponding increase in aptamer-PSA complexes, resulting in decreased activation of CRISPR/Cas12a systems and ultimately fewer cleaved ssDNA strands. This demonstrates the

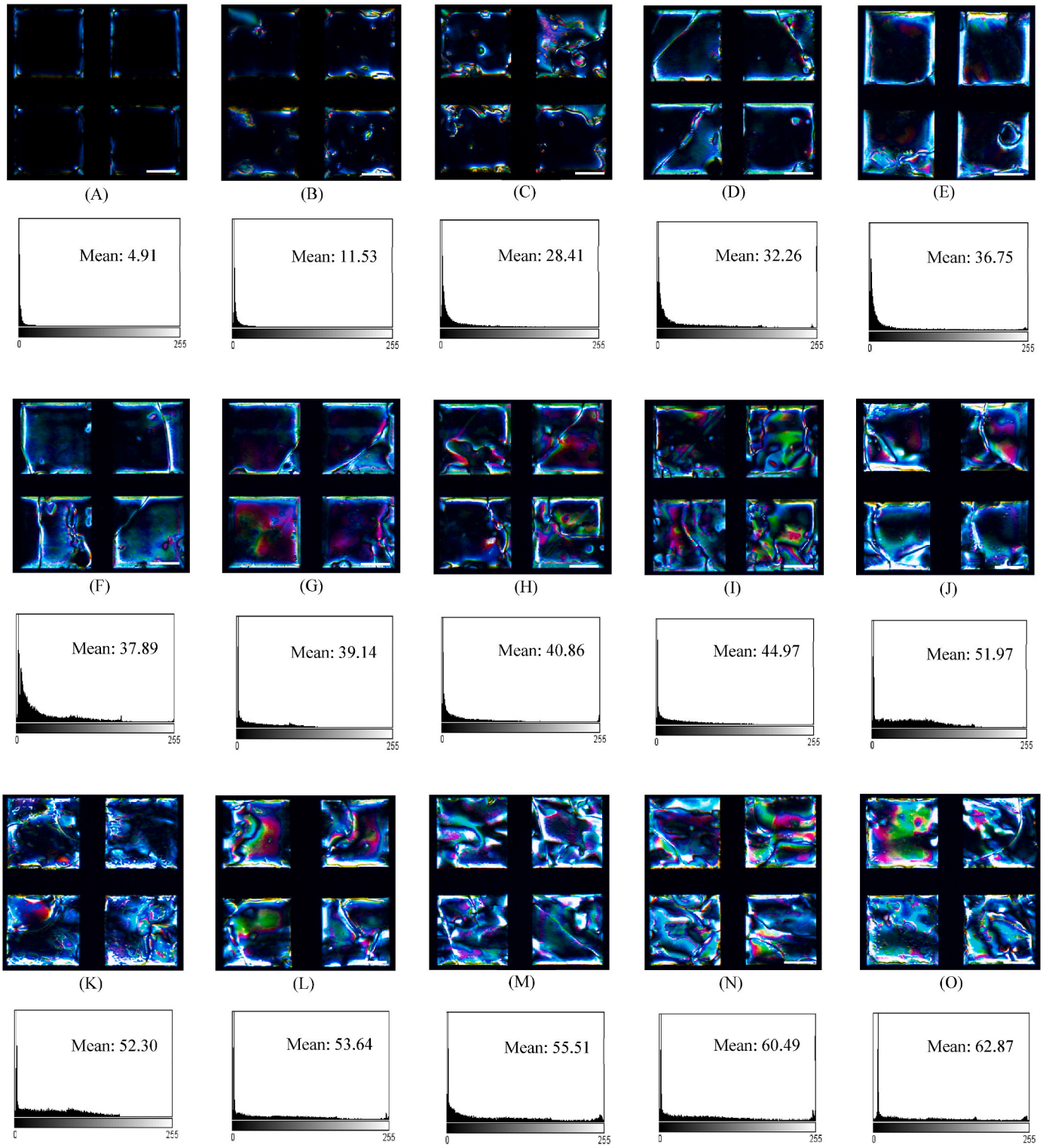


Fig. 1. The polarized view of the LC aptasensor powered by CRISPR/Cas12a system upon addition of different PSA quantities: (A) 0 ag mL^{-1} (blank sample); (B) 1 ag mL^{-1}; (C) 100 ag mL^{-1}; (D) 1 fg mL^{-1}; (E) 10 fg mL^{-1}; (F) 100 fg mL^{-1}; (G) 200 fg mL^{-1}; (H) 400 fg mL^{-1}; (I) 1 pg mL^{-1}; (J) 10 pg mL^{-1}; (K) 100 pg mL^{-1}; (L) 200 pg mL^{-1}; (M) 400 pg mL^{-1}; (N) 800 pg mL^{-1}; (O) 1 ng mL^{-1}. Scale bar: 100 μm. The related surface plots are shown in Fig. S11.

superior performance of the newly developed aptasensor, which induces a colorimetric change on the glass platform.

In the context of quantitative analysis, the average Gray parameter as a criterion of the darkness of the aptasensing substrate in the presence of the different PSA concentrations was computed by ImageJ software as presented in the SI, and inversely correlated with the mean brightness parameter; so that the higher the Mean Gray value, the less the mean brightness parameter and the higher the platform's darkness. A calibration curve was created to show the relationship between the average Gray parameter and PSA levels ranging from 1 ag mL^{-1}–1 ng mL^{-1} (Fig. 2). The mean Gray parameter was proportional to the PSA concentration with a regression equation as follows:

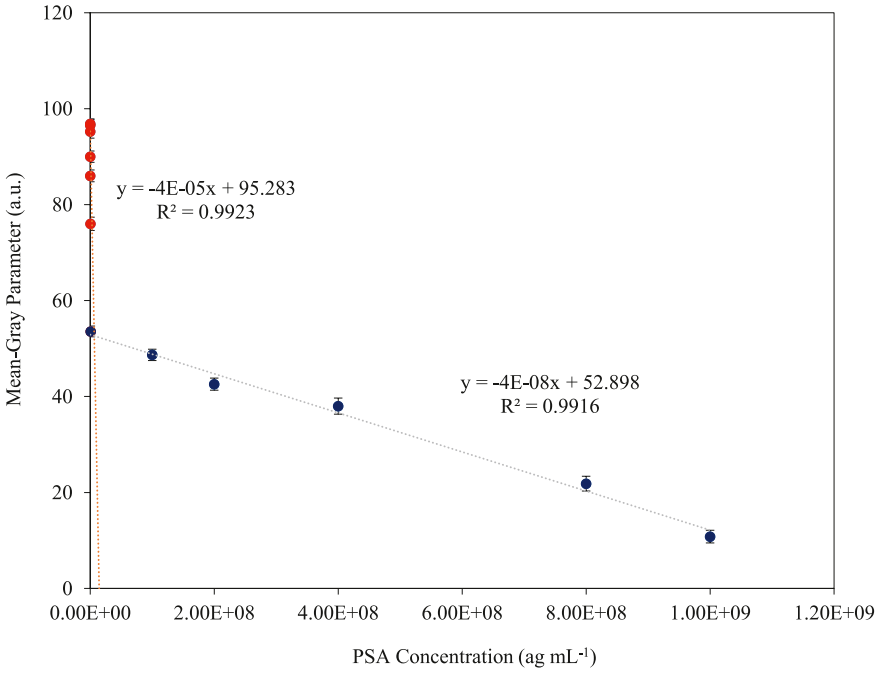


Fig. 2. The calibration curve of the Mean Gray factor and PSA quantity (n = 3).

Mean-Gray Parameter (a.u.) = −4 × 10^-5 (±2.16 × 10^-8) [PSA] (ag/mL) + 95.28 (±0.02); R^2 = 0.992 in the PSA concentration range of 1 pg mL^{-1}–1 ng mL^{-1}

Mean-Gray Parameter (a.u.) = −4 × 10^-8 (±4.71 × 10^-11) [PSA] (ag/mL) + 52.90 (±0.06); R^2 = 0.992 in the range of 1 pg mL^{-1}–1 ng mL^{-1}

Besides, the detection limit (LOD) was computed 0.28 ag mL^{-1} according to the literature (Schmitteckert and Schlicht, 1999) by using the formula of $3\sigma S^{-1}$ (S and σ are the slope of the calibration curve and standard deviation of control sample, respectively). Consequently, the proposed aptasensor can be an efficient diagnostic tool in the field of healthcare monitoring.

To further validate the effective development of the aptasensor, its functionality was evaluated utilizing the agarose gel electrophoresis technique (2.5 %). Fig. S12 illustrates the unaltered band of ssDNA alongside the slowed band for the PSA/Aptamer conjugate (lane 4) in contrast to the individual strands of the specific aptamer (lane 1). This observation is attributed to the increase in molecular weight of the aptamer following its interaction with PSA within the CRISPR/Cas12a system, which comprises crRNA, aptamer, and ssDNA strands in the presence of PSA (1 ng mL^{-1}). This finding confirms the inhibition of the cleavage activity of the CRISPR/Cas12a complex when the target is present. Conversely, the absence of the ssDNA band (Lane 5) for the CRISPR/Cas12a system that includes crRNA, aptamer, and ssDNA strands without PSA corroborates the catalytic capability of the CRISPR/Cas12a system for trans-cleaving ssDNA strands.

As another confirmation, the surface topography of the platform was analyzed at various stages of preparation. This included the modification with APTES/DMOAP mixture, binding of ssDNA strand, activation of CRISPR/Cas12a system, and interaction with inactivated CRISPR/Cas12a in the presence of PSA, as depicted in Fig. S13. Significantly, the platform roughness increased after attaching ssDNA strand on it. By exerting activated CRISPR/Cas12a assembly, the roughness of the platform surface decreased impressively, proving the high efficiency of CRISPR/Cas12a system for the cleavage of ssDNA strands. In the presence of PSA, the platform roughness was almost the same as that obtained for the modified surface with ssDNA sequence. It confirmed maintaining of the strands on the surface in the presence of PSA through inactivation of CRISPR/Cas12a assembly.

The aptasensor capability for sensitive monitoring of PSA biomarker was compared to some previously developed aptasensors, as summarized in Table S3. Table S3 highlights the superiority of the developed LC aptasensor in the term of sensitivity rather than the others. Obviously, nanoparticle-tuned aptasensors could monitor PSA in the nanomolar levels. While the LC aptasensor could identify PSA in the concentration range of attomolar to nanomolar with no involvement of nanoparticles, which converts it to a cost-effective, simple, and facile-to-operate sensing approach. In our recent study (Khoshbin et al., 2023b), we produced a simple and low-cost LC-included aptasensor to detect PSA levels based on the orientational variation of LCs in the surfactant-ordered interface. The LC aptasensor that was developed earlier was able to detect PSA in concentrations ranging from 1 to 1200 pg mL^{-1} with a detection limit of 0.148 pg mL^{-1}. By combining CRISPR technology with the LC aptasensing strategy, PSA detection at attomolar levels was achieved, showing great potential for early-stage cancer diagnosis.

3.4. Selectivity test

The aptasensor response toward some other biomarkers as the interference compounds including SNCA, HSA, cTnI, AFP, Mb, TH, rCRP, and SST was investigated to prove its selective response. Fig. 3 indicates the polarized aptasensing platform in the presence of the different biomarkers in the buffer medium. A relatively dark background of the aptasensor was obtained in the presence of the interferences, clarifying the right function of CRISPR/Cas12a assembly activated by the free aptamers for cleaving ssDNA strands. While PSA formed a complex with the specific aptamer, which inactivated CRISPR/Cas12a assembly, resulting in a multicolored sensing platform. As a consequence, the CRISPR/Cas12a-powered LC aptasensor could detect PSA selectively.

3.5. Spiked sample analysis

The aptasensor feasibility for PSA detection in complex biological

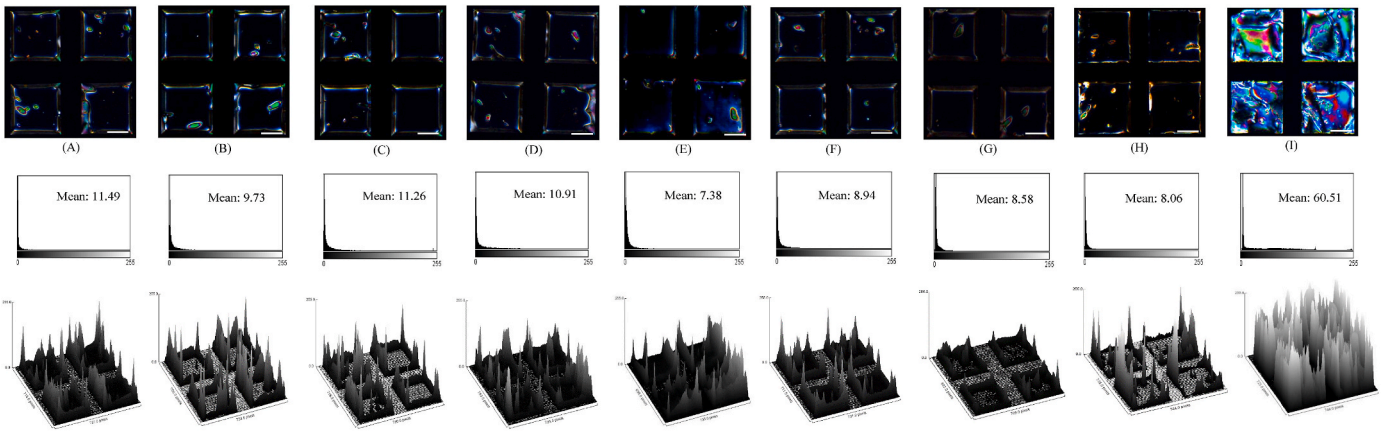


Fig. 3. The CRISPR/Cas12a-powered LC aptasensor was analyzed quantitatively in the presence of various biomarkers, namely A) HSA, B) TH, C) SST, D) cTnI, E) Mb, F) rCRP, G) AFP, H) SNCA, I) PSA (The concentration in each sample: 800 pg mL^{-1}) in the buffer medium. Scale bar: 100 μm.

matrix was tested in human serum samples. The aptasensor was used to analyze spiked human serum samples (taken from a healthy man, age = 42) containing various concentrations of PSA. The polarized images, mean brightness values, and surface plots are shown in Fig. S14; and the quantitative findings are presented in Table 1. The obtained recovery values ranged from 96.10 % to 99.02 %, affirming the effectiveness of the aptasensor for clinical use as a reliable diagnostic tool.

To validate the aptasensing assay for measuring PSA in serum samples, its accuracy was examined against an accepted laboratory method (Immunoassay system). The results are given in Table 2. Based on Table 2, the developed aptasensor can be an accurate assay for highly sensitive detection of PSA levels in both cancerous human serum as the real samples and spiked ones.

3.6. Reproducibility and stability tests

In order to validate the reproducibility of the developed aptasensor, its reaction was evaluated in the presence of PSA on three separate days, involving three repeated measurements. Fig. S15 illustrates that the aptasensor exhibited a consistently similar response both in the absence and presence of PSA across the three different days, with an insignificant coefficient of variation (CV) of 0.010 and 0.011, and relative standard deviation (RSD) values of 0.0020 and 0.0009, respectively. These findings confirm the excellent reproducibility of the aptasensor.

To assess its stability, the aptasensor treated with PSA (1 ag mL^{-1}) was stored at a temperature of 4 °C for varying durations (24, 48, and 72 h), and polarized images were captured for quantitative evaluation. Fig. S16 presents the polarized image of the aptasensor along with the corresponding quantitative results. According to Fig. S16, the brightness of the aptasensor remained stable for 48 h, exhibiting only a slight decrease of approximately 0.17 %. However, a significant reduction in brightness was observed after 72 h. Therefore, the LC aptasensor demonstrates reliable functionality and satisfactory stability over a period of 48 h.

4. Conclusion

For the first time, we designed a promising CRISPR/Cas12a incorporated LC aptasensor to monitor the ultralow levels of PSA. By examining the arrangement of LCs guided by the fixed ssDNA molecules serving as an orientation controller of LCs on the detection surface following the enzymatic action of CRISPR/Cas12a complex, the levels of PSA could be accurately measured. So that, the presence of PSA inactivated the cleavage function of CRISPR/Cas12a assembly for shredding ssDNA sequences, resulting in disordered orientation of LCs and subsequently, a multicolor polarized view of the sensing substrate. A change in the polarized view of the aptasensor substrate was used to monitor PSA in the concentration ranging from 1 ag mL^{-1}–1 ng mL^{-1} with the LOD of 0.28 ag mL^{-1}. Based on its ability to detect PSA in the spiked and real human serum samples, the developed approach is effective in the field of cancer diagnosis and treatment. With providing the superiorities of high sensitivity, facility, easy-to-operate, and cost-effective, the proposed aptasensor can be upgraded as a portable gadget for on-site monitoring of PSA by using a handheld polarized light microscope. However, applying the aptasensor in a high-temperature laboratory environment is restricted due to loss of the contrast of LC molecules. Besides, bright texture of LCs limits application of the developed aptasensor in laboratory with lots of light (O'Neill and Kelly, 2003; Pagano-Stauffer et al., 1986). Hence, designing an LC-based aptasensor with peripherals useable in inhibitory environmental conditions (high

Table 1
PSA levels were quantified in the spiked samples by using the CRIPR/Cas12a powered LC aptasensor (n = 3).

Sample	Found Initial PSA[a] (ng mL^{-1})	Found Initial PSA[b] (ng mL^{-1})	Added PSA (ng mL^{-1})[a]	Total Recovered PSA (ng mL^{-1})[c]	Total Recovered PSA (ng mL^{-1})[d]	Total Recovered PSA (ng mL^{-1})[e]	Mean of Total Recovered PSA (ng mL^{-1})[f]	Recovery (%)	RSD (%, n = 3)[g]
1	0.69	0.65	0.01	0.638	0.651	0.648	0.646	97.83	1.05
2	0.69	0.65	0.05	0.669	0.671	0.678	0.673	96.10	0.70
3	0.69	0.65	0.1	0.748	0.742	0.738	0.743	99.02	0.68
4	0.69	0.65	0.2	0.821	0.835	0.846	0.834	98.12	1.50

[a] Measured by Immunoassay system.
[b] Measured by the aptasensor.
[c] Measured PSA from test 1.
[d] Measured PSA from test 2.
[e] Measured PSA from test 3.
[f] Average value of three recovered PSA amounts.
[g] Obtained by dividing the standard deviation of three recovered PSA amounts to mean of total recovered value, multiplied to 100.

Table 2
PSA levels were measured in the real and spiked samples by using the LC aptasensor and IMMULITE 2000 Immunoassay system.

No.	Source of Sample[a]	Age of Candidate	Real/Spiked Type	Spiked PSA Amount (ng mL^{-1})	Measured by Immunoassay system (ng mL^{-1})	Measured by Aptasensor[b] (ng mL^{-1})
1	Cancerous patient	64	Real	0	35.1	35.351
2	Cancerous patient	64	Real	0	15.9	16.128
3	Cancerous patient	56	Real	0	>100	106.841
4	Healthy person	32	Real	0	2.7	2.816
5	Healthy person	32	Spiked in sample 4	5	8.3	7.725
6	Healthy person	32	Spiked in sample 4	100	96.3	102.841

[a] The volunteers' name is not permitted to be mentioned.
[b] Since the aptasensor can quantify PSA levels in the ranges of 1 ag mL^{-1}–1 pg mL^{-1} and 1 pg mL^{-1}–1 ng mL^{-1}, appropriate dilution process was applied based on the upper threshold of the aptasensor linear range (1 ng mL^{-1}).

temperature and light) could be a goal for future studies.

CRediT authorship contribution statement

Zahra Khoshbin: Writing – original draft, Investigation, Conceptualization. **Elham Sameiyan:** Writing – review & editing, Investigation. **Fatemeh Alizadeh:** Writing – review & editing, Resources, Investigation. **Mohammad Ramezani:** Writing – review & editing, Methodology. **Mona Alibolandi:** Writing – review & editing, Formal analysis. **Khalil Abnous:** Writing – review & editing, Supervision, Funding acquisition, Conceptualization. **Seyed Mohammad Taghdisi:** Writing – review & editing, Validation, Project administration, Conceptualization.

Declaration of competing interest

The authors declare that they have no known competing financial interests or personal relationships that could have appeared to influence the work reported in this paper.

Acknowledgment

This study is financed by Iran National Science Foundation (INSF) as a research project (Project 4004894). Ethic number: IR.MUMS.PHARMACY.REC.1401.058.

Appendix A. Supplementary data

Supplementary data to this article can be found online at https://doi.org/10.1016/j.bios.2025.117651.

Data availability

Data will be made available on request.

References

Abnous, K., Danesh, N.M., Ramezani, M., Alibolandi, M., Nameghi, M.A., Zavvar, T.S., Taghdisi, S.M., 2021a. A novel colorimetric aptasensor for ultrasensitive detection of aflatoxin M1 based on the combination of CRISPR-Cas12a, rolling circle amplification and catalytic activity of gold nanoparticles. Anal. Chim. Acta 1165, 338549.

Abnous, K., Danesh, N.M., Ramezani, M., Alibolandi, M., Nameghi, M.A., Zavvar, T.S., Taghdisi, Seyed Mohammad, 2021b. A Novel Colorimetric Aptasensor for Ultrasensitive Detection of Aflatoxin M1 Based on the Combination of CRISPR-Cas12a, Rolling Circle Amplification and Catalytic Activity of Gold Nanoparticles, vol.1165, 338549.

Adamaki, M., Zoumpourlis, V., 2021. Prostate cancer biomarkers: from diagnosis to prognosis and precision-guided therapeutics. Pharmacol. Therapeut. 228, 107932.

Benvidi, A., Banaei, M., Tezerjani, M.D., Molahosseini, H., Jahanbani, S., 2018. Impedimetric PSA aptasensor based on the use of a glassy carbon electrode modified with titanium oxide nanoparticles and silk fibroin nanofibers. Microchim. Acta 185, 1–10.

Charbgoo, F., Soltani, F., Taghdisi, S.M., Abnous, K., Ramezani, M., 2016. Nanoparticles application in high sensitive aptasensor design. TrAC, Trends Anal. Chem. 85, 85–97.

Chen, Q., Gao, H., Yao, J., Jiang, B., Yuan, R., Xiang, Y., 2023. Target/Aptamer binding-induced inhibition of enzyme activity for amplified electrochemical detection of sonic hedgehog protein. Sens. Actuators B: Chem. 385, 133702.

Cheng, Z., Choi, N., Wang, R., Lee, S., Moon, K.C., Yoon, S.-Y., Chen, L., Choo, J.J.A.N., 2017. Simultaneous detection of dual prostate specific antigens using surface-enhanced raman scattering-based immunoassay for accurate diagnosis of prostate cancer, 11 (5), 4926–4933.

Cong, L., Ran, F.A., Cox, D., Lin, S., Barretto, R., Habib, N., Hsu, P.D., Wu, X., Jiang, W., Marraffini, L.A.J.S., 2013. Multiplex genome engineering using CRISPR/cas systems, 339 (6121), 819–823.

Cong, L., Zhang, F.J.C.m., 2015. Genome Engineering Using CRISPR-Cas9 System, pp. 197–217.

Cui, L., Wu, J., Ju, H., 2016. Label-free signal-on aptasensor for sensitive electrochemical detection of arsenite. Biosens. Bioelectron. 79, 861–865.

Dadmehr, M., Shahi, S.C., Malekkiani, M., Korouzhdehi, B., Tavassoli, A., 2023. A stem-loop like aptasensor for sensitive detection of aflatoxin based on graphene oxide/AuNPs nanocomposite platform. Food Chem. 402, 134212.

Dehghani, S., Danesh, N.M., Ramezani, M., Alibolandi, M., Lavaee, P., Nejabat, M., Abnous, K., Taghdisi, S.M., 2018. A label-free fluorescent aptasensor for detection of kanamycin based on dsDNA-capped mesoporous silica nanoparticles and rhodamine B. Anal. Chim. Acta 1030, 142–147.

Deng, F., Li, Y., Li, B., Goldys, E.M., 2022. Increasing trans-cleavage catalytic efficiency of Cas12a and Cas13a with chemical enhancers: application to amplified nucleic acid detection. Sensor. Actuator. B Chem. 373, 132767.

Edwards, B.K., Brown, M.L., Wingo, P.A., Howe, H.L., Ward, E., Ries, L.A., Schrag, D., Jamison, P.M., Jemal, A., X.C.J.J.o.t.N.C.I. Wu, 2005. Annual report to the nation on the status of cancer, 1975–2002, featuring population-based trends in cancer treatment, 97 (19), 1407–1427.

Etzioni, R., Urban, N., Ramsey, S., McIntosh, M., Schwartz, S., Reid, B., Radich, J., Anderson, G., Hartwell, L., 2003. The case for early detection. Nat. Rev. Cancer 3 (4), 243–252.

Fang, X., 2010. Aptamers generated from cell-SELEX for molecular medicine: a chemical biology approach. Acc. Chem. Res. 43 (1), 48–57. W Tan.

Forouzanfar, S., Alam, F., Pala, N., Wang, C., 2020. Highly sensitive label-free electrochemical aptasensors based on photoresist derived carbon for cancer biomarker detection. Biosens. Bioelectron. 170, 112598.

Gorgani, L., Mohammadi, M., Darzi, G.N., Raoof, J.B., 2023. Electrochemical aptasensor based on bimetallic CuZr-MOF for ultrasensitive detection of miR-21. Sensor. Actuator. B Chem. 378, 133194.

Graves, H., Wehner, N., Stamey, T.A.J.C.c., 1992. Ultrasensitive radioimmunoassay of prostate-specific antigen, 38 (5), 735–742.

Hajikhani, M., Zhang, Y., Gao, X., Lin, M., 2023. Advances in CRISPR-Based SERS detection of food contaminants: a review. Trends Food Sci. Technol. 138, 615–627.

Haowei, M., Ebrahimi, S., Mansouri, S., Shukhratovich Abdullaev, S., Alsaab, H.O., Hassan, Z.F., 2023. CRISPR/Cas-based nanobiosensors: a reinforced approach for specific and sensitive recognition of mycotoxins. Food Biosci. 56, 103110.

Hussain, Z., Qazi, F., Ahmed, M.I., Usman, A., Riaz, A., Abbasi Bioelectronics, A.D.J.B., 2016. Liquid Crystals Based Sensing platform-technological Aspects, vol. 85, pp. 110–127.

Jia, M., Sha, J., Li, Z., Wang, W., Zhang, H., 2020. High affinity truncated aptamers for ultra-sensitive colorimetric detection of bisphenol A with label-free aptasensor. Food Chem. 317, 126459.

Kadam, U.S., Cho, Y., Park, T.Y., Hong, Jong Chan, 2023. Aptamer-based CRISPR-cas powered diagnostics of diverse biomarkers and small molecule targets, 66 (1), 1–15.

Khoshbin, Z., Abnous, K., Taghdisi, S.M., Verdian, A., Sameiyan, E., Ramezani, M., Alibolandi, M.J.F.C., 2022a. An Ultra-sensitive dual-responsive Aptasensor with Combination of Liquid Crystal and Intercalating Dye Molecules: a Food Toxin Case study, vol. 381, 132265.

Khoshbin, Z., Verdian, A., Taghdisi, S.M., Danesh, N.M., Abnous, K., 2023a. A novel liquid crystal assay based on aptazyme-assisted bioprobe for ultra-sensitive monitoring of lead ion. Sensor. Actuator. B Chem. 375, 132926.

Khoshbin, Z., Zahraee, H., Ramezani, M., Alibolandi, M., Verdian, A., Abnous, K., Taghdisi, S.M., 2023b. Surfactant-regularized liquid crystal aptasensor for optical monitoring of prostate-specific antigen: appropriate for health care monitoring. Microchem. J. 193, 109002.
Khoshbin, Z., Zahraee, H., Zamanian, J., Verdian, A., Ramezani, M., Alibolandi, M., Abnous, K., Taghdisi, S.M., 2022b. A label-free liquid crystal-assisted aptasensor for trace level detection of tobramycin in milk and chicken egg samples. Anal. Chim. Acta 1236, 340588.
Kim, H.J., Jang, C.-H.J.S., Chemical, A.B., 2019. Liquid Crystal-based Aptasensor for the Detection of interferon-γ and Its Application in the Diagnosis of Tuberculosis Using Human Blood, vol. 282, pp. 574–579.
Lee, J.H., Yigit, M.V., Mazumdar, D., 2010. Molecular diagnostic and drug delivery agents based on aptamer-nanomaterial conjugates. Adv. Drug deliv. rev. 62 (6), 592–605. Y Lu.
Li, H., Cai, Q., Wang, J., Jie, G., 2023. Versatile FeMoOv nanozyme bipolar electrode electrochemiluminescence biosensing and imaging platform for detection of H2O2 and PSA. Biosens. Bioelectron. 232, 115315.
Li, H., Wei, Q., He, J., Li, T., Zhao, Y., Cai, Y., Du, B., Qian, Z., Yang, M.J.B., 2011. Bioelectronics. Electrochemical immunosensors for cancer biomarker with signal amplification based on ferrocene functionalized iron oxide nanoparticles, 26 (8), 3590–3595.
Li, S.-Y., Cheng, Q.-X., Liu, J.-K., Nie, X.-Q., Zhao, G.-P., Wang, J.J.C.r., 2018. CRISPR-Cas12a has both cis-and trans-cleavage activities on single-stranded. DNA (N. Y.) 28 (4), 491–493.
Li, Z., Yin, J., Gao, C., Qiu, G., Meng, A., Li, Q., 2019. The construction of electrochemical aptasensor based on coral-like poly-aniline and Au nano-particles for the sensitive detection of prostate specific antigen. Sensor. Actuator. B Chem. 295, 93–100.
Lilja, H., Ulmert, D., Vickers, A.J., 2008. Prostate-specific antigen and prostate cancer: prediction, detection and monitoring. Nat. Rev. Cancer 8 (4), 268–278.
Ludwig, J.A., 2005. Biomarkers in cancer staging, prognosis and treatment selection. Nat. Rev. Cancer 5 (11), 845–856. JN Weinstein.
Ma, K., Li, X., Xu, B., Tian, W., 2021. Label-free bioassay with graphene oxide-based fluorescent aptasensors: a review. Anal. Chim. Acta 1188, 338859.
Madu, C.O., Lu, Y.J.J.o.C., 2010. Novel diagnostic biomarkers for prostate cancer, 1, 150.
Mohammadi, F., Khoshbin, Z., Ramezani, M., Alibolandi, M., Abnous, K., Taghdisi, S.M., Moeenfard, M., 2024a. A simple label-free aptasensor for acrylamide monitoring using a four-way arm junction structure of DNA strands. Microchem. J. 199, 110215.
Mohammadi, F., Zahraee, H., Izadpanah Kazemi, M., Habibi, Z.S., Taghdisi, S.M., Abnous, K., Khoshbin, Z., Chen, C.-H., 2024b. Recent advances in aptamer-based platforms for cortisol hormone monitoring. Talanta 266, 125010.
Nakhjavani, S.A., Tokyay, B.K., Soylemez, C., Sarabi, M.R., Yetisen, A.K., Tasoglu, S., 2023. Biosensors for prostate cancer detection. Trends Biotechnol.
Nandi, R., 2018. Liquid crystal based sensing device using a smartphone. Analyst 143 (5), 1046–1052. SK Pal.
Nguyen, T.T.-Q., Gu, M.B., 2023. An ultrasensitive electrochemical aptasensor using Tyramide-assisted enzyme multiplication for the detection of Staphylococcus aureus. Biosens. Bioelectron. 228, 115199.
O'Neill, M., Kelly, S.M., 2003. Liquid crystals for charge transport, luminescence, and photonics. Adv. Mater. 15 (14), 1135–1146.
Pagano-Stauffer, L.A., Johnson, K.M., Masterson, H.J., Clark, N.A., Handschy, M.A., 1986. Optical logic gates using ferroelectric liquid crystals. OSA Annual Meeting. Optica Publishing Group, p. FG2.
Sánchez-Salcedo, R., Gómez-Meijide, P., Miranda-Castro, R., de-los-Santos-Álvarez, N., Lobo-Castañón, M.J., 2022. Electrochemical sensors using oligonucleotides as recognition ligands for liquid biopsy in prostate cancer. Biosens. Bioelectron. X 12, 100227.
Savory, N., Abe, K., Sode, K., Ikebukuro, K., 2010. Selection of DNA aptamer against prostate specific antigen using a genetic algorithm and application to sensing. Biosens. Bioelectron. 26 (4), 1386–1391.
Schmitteckert, E.M., Schlicht, H.-J., 1999. Detection of the human hepatitis B virus X-protein in transgenic mice after radioactive labelling at a newly introduced phosphorylation site. J. Gen. Virol. 80 (9), 2501–2509.
Sekhoacha, M., Riet, K., Motloung, P., Gumenku, L., Adegoke, A., Mashele, S., 2022. Prostate cancer review: genetics, diagnosis, treatment options, and alternative approaches. Molecules 27 (17), 5730.
Song, Z., Song, J., Gao, F., Chen, X., Wang, Q., Zhao, Y., Huang, X., Yang, C., Wang, Q., 2022. Novel electroactive ferrocene-based covalent organic frameworks towards electrochemical label-free aptasensors for the detection of cardiac troponin I. Sensor. Actuator. B Chem. 368, 132205.
Souada, M., Piro, B., Reisberg, S., Anquetin, G., Noël, V., Pham, M.C., 2015. Label-free electrochemical detection of prostate-specific antigen based on nucleic acid aptamer. Biosens. Bioelectron. 68, 49–54.
Srivastava, M., Nirala, N.R., Srivastava, S., Prakash, R.J.S.r., 2018. A comparative study of aptasensor vs immunosensor for label-free PSA cancer detection on GQDs-AuNRs modified screen-printed electrodes, 8 (1), 1923.
Syga, Ł., Spakman, D., Punter, C.M., Poolman, B., 2018. Method for immobilization of living and synthetic cells for high-resolution imaging and single-particle tracking. Sci. Rep. 8 (1), 13789.
Taghdisi, S.M., Danesh, N.M., Nameghi, M.A., Ramezani, M., Alibolandi, M., Abnous, K., 2020a. A DNA triangular prism-based fluorescent aptasensor for ultrasensitive detection of prostate-specific antigen. Anal. Chim. Acta 1120, 36–42.
Taghdisi, S.M., Danesh, N.M., Nameghi, M.A., Ramezani, M., Alibolandi, M., Abnous, K., 2020b. A DNA Triangular Prism-based Fluorescent Aptasensor for Ultrasensitive Detection of Prostate-specific Antigen, vol 1120, pp. 36–42.
Taghdisi, S.M., Ramezani, M., Alibolandi, M., Khademi, Z., Hajihasani, M.M., Alinezhad Nameghi, M., khakshour Abdolabadi, A., Rahimi, H., Abnous, K., Danesh, N.M., 2022a. A highly sensitive fluorescent aptasensor for detection of prostate specific antigen based on the integration of a DNA structure and CRISPR-Cas12a. Anal. Chim. Acta 1219, 340031.
Taghdisi, S.M., Ramezani, M., Alibolandi, M., Khademi, Z., Hajihasani, M.M., Alinezhad Nameghi, M., khakshour Abdolabadi, A., Rahimi, H., Abnous, K., Danesh, N.M., 2022b. A highly sensitive fluorescent aptasensor for detection of prostate specific antigen based on the integration of a DNA structure and CRISPR-Cas12a. Anal. Chim. Acta 1219, 340031.
Verdian, A., Khoshbin, Z., Chen, C.-H., 2022. Development of a novel liquid crystal Apta-sensing platform using P-shape molecular switch. Biosens. Bioelectron. 199, 113882.
Verdian, A., Khoshbin, Z., Chen, C.-H., Hu, Q., 2023. Attomolar analyte sensing technique for detection of Pb2+ and Hg2+ ions based on liquid crystal. Talanta 253, 124042.
Wang, Y., Wang, B., Shen, J., Xiong, X., Deng, S.J.M.A., 2017. Aptamer Based Bare Eye Detection of Kanamycin by Using a Liquid Crystal Film on a Glass Support, vol. 184, pp. 3765–3771.
Wei, J., Liu, Z., Zhang, Z., Lan, K., Wang, Y., Chen, R., Qin, G., 2023. Suspended CNTs/MoS2 heterostructure field effect transistor for high performance biosensor and its application for serum PSA detection. Sensor. Actuator. B Chem. 381, 133417.
Wu, C.-C., Manga, Y.B., Yang, M.-H., Chien, Z.-S., Lee, K.-S., 2018. Label-free detection of BRAFV599E gene mutation using side-gated nanowire field effect transistors. J. Electrochem. Soc. 165 (13), B576.
Wu, Z., Sun, D.-W., Pu, H., Wei, Q.J.T., 2023. A Novel Fluorescence Biosensor Based on CRISPR/Cas12a Integrated Mxenes for Detecting Aflatoxin B1, vol. 252, 123773.
Xuan, Z., Li, M., Rong, P., Wang, W., Li, Y., Liu, D.J.N., 2016. Plasmonic ELISA based on the controlled growth of silver nanoparticles, 8 (39), 17271–17277.
Zavvar, T.S., Khoshbin, Z., Ramezani, M., Alibolandi, M., Abnous, K., Taghdisi, S.M., 2022. CRISPR/Cas-engineered technology: innovative approach for biosensor development. Biosens. Bioelectron. 214, 114501.
Zhang, J., Su, X., Yang, D., Luan, C.J.T., 2018. Label-Free Liquid Crystal Biosensor for Cecropin B Detection, vol. 186, pp. 60–64.